

Finite Element Analysis on the Elastic Contact between a Donut-Shaped Asperity and a Half-Space

Jiunn-Jong Wu* and Chia-Hung Wu**

Keywords: contact mechanics, donut-shaped asperity

Abstract

The contact for donut-shaped asperity has been investigated for decades based on two-dimensional Hertz contact. In this paper, the contact is investigated by finite element analysis. The results show that two-dimensional Hertz contact can predict the contact only for the donut-asperity with large radius. Thus, new semi-empirical equations are proposed. The total load, load-indentation depth relations and the coordinates of contact edges can be predicted accurately by semi-empirical equations. For the donut-asperity with small radius, the modified model can predict the contact.

Introduction

Laser texturing is important for surface engineering. Laser texturing is important for surface engineering. It is usually used for metallic materials in micro/nano scale due to the focal size of laser pulses (Dou et al., 2023). It can produce surfaces with various wettability, adhesion and friction properties (Bhaduri et al. 2017). The laser texturing can be used in the touchdown area of computer hard-disks to avoid the stiction problem (Gui et al., 1997). It can also be used in aerospace, marine and biomedical industries (Dou et al., 2023) and engine component (Rossi and Vieira, 2019). The asperities made by laser texturing have an annular shapes consisting of a crater surrounded by a raised rim. These may be called “volcano” or “donut” type bumps (Oka, 2000) (which

is called the donut-shaped asperity in this paper). The contact of such asperities was investigated for decades.

Gui et al. (1997) investigated the stiction of the donut-shaped asperity experimentally. They propose a stiction model by fitting the experimental results. Zhao and Talke (2000) investigated the plasticity index for the contact of the donut-shaped asperities. The asperity in their model is like a real baker's donut. Their model is based on the contact between the circular-cylinder and a half-space. Oka (2000) proposed an analytical solution for the contact of the donut-shaped asperity based on the point Hertz contact. His solution can be evaluated numerically using double integrals. However, his solution needs very complicated computation. Therefore, assuming the initial shape along any radial line is parabolic, Greenwood (2001) solved this problem based on the two-dimensional Hertz contact. Greenwood proposed easy-implemented equations. Argatov et al. (2016) also used two-dimensional Hertz contact to perform a study of toroidal indenters. They used the leading-order asymptotic solution for the contacts of the power-law shaped torus, and obtained the same as Greenwood (2001) for donut-shaped torus.

All previous researches are based on the point-Hertz contact or two-dimensional Hertz contact, and are not accurate. The correct prediction for donut-shaped asperity contact is important. If the accuracy is not enough, engineering problem (e.g. stiction) may occur. (Gui et al., 1997). Therefore, the contact for donut asperity is investigated using finite element method (Kelly et al., 2022) or experiment (Dou et al., 2023) recently. In this paper, the contact of the donut asperity is investigated using finite element method. The more accurate results are obtained. The results are compared with Greenwood's research (2001). New semi-empirical equations are proposed.

Analyses

1. Model

The contact between a donut-shaped asperity and a half-space is shown in Figure 1. The asperity is annular, and is approximated parabolic shape in its

*Paper Received September, 2021. Revised September, 2022.
Accepted January, 2023. Author for Correspondence: Jiunn-Jong Wu.*

* Professor, Department of Mechanical Engineering, Chang Gung University, TaoYuan, Taiwan 33302, ROC.

** Graduate Student, Institute of Applied Mechanics, National Taiwan University, Taipei, Taiwan 10617, ROC.

cross section. The asperity is pushed towards an elastic half-space. The contact is elastic and frictionless. The elastic contact between an asperity and a half-space can be regarded as the contact between a rigid asperity and an elastic half-space. Thus, the donut-shaped asperity is set to be rigid.

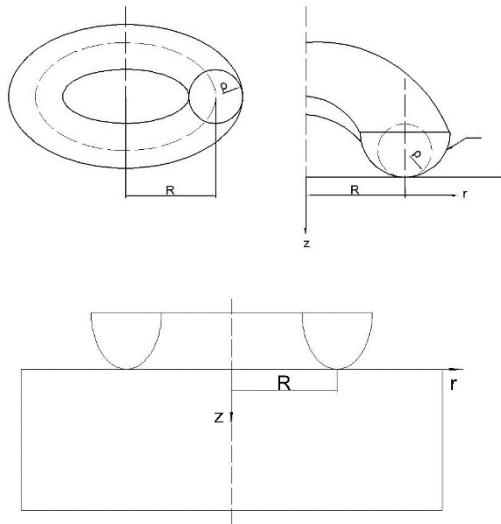


Figure 1. The contact between a donut and a half-space.

In this research, the cylindrical coordinate system is used. As shown in Fig. 1, the radius of the annular donut is R . The cross section of the donut-shaped asperity is assumed to be parabolic with radius of curvature equal to ρ . When in contact, the contact half-width is b . In the laser texture asperity, $\rho \gg R$. In Greenwood's research (2001), the contact for $\rho = 10R$ was investigated. In this research, the contacts for $R = 0.1\rho, 0.2\rho, 0.4\rho$ and ρ ($R/\rho = 0.1, 0.2, 0.4, 1$) are investigated.

2. Greenwood's research

Greenwood (2001) assumed that the pressure distribution at the cross section of the contact follows that of the two-dimensional Hertz contact,

$$p = \frac{p_0}{b} \sqrt{b^2 - (r - R)^2} \quad (1)$$

where r is the radial coordinate and p_0 is the maximum pressure. Thus, the indentation depth δ is derived.

$$\delta = \frac{bp_0}{E^*} \left(\ln \frac{16R}{b} + \frac{1}{2} \right) \quad (2)$$

where $E^* = (1 - \nu^2)/E$ is the equivalent Young's modulus (while E is Young's modulus and ν is Poisson ratio of the elastic half-space.). Argatov et al. (2016) used different approach and obtained the same result.

In two-dimensional Hertz contact, the maximum pressure p_0 and the total load W have the following relationships.

$$p_0 = \frac{bE^*}{2\rho} \quad (3)$$

$$W = \pi^2 R b p_0 \quad (4)$$

Thus, equation (2) can also expressed as

$$\delta = \frac{b^2}{2\rho} \left(\ln \frac{16R}{b} + \frac{1}{2} \right) \quad (5)$$

$$\delta = \frac{W}{\pi^2 R E^*} \left(\ln \frac{16R}{b} + \frac{1}{2} \right) \quad (6)$$

Greenwood (2001) found that, given δ , ρ and R , the contact half-width b can be obtained from equation (5) by iteration. Thus, p_0 , p and W can be obtained by equations (3), (1) and (4), respectively.

By fitting the experimental stiction results, Gui et al. (1997) obtained a similar equation with a different constant.

$$\delta = \frac{W}{\pi^2 R E^*} \left(\ln \frac{8\pi R}{b} - 0.1935 \right) \quad (7)$$

Zhao and Talke (2000) using a different approach and obtained a totally different equation.

$$\delta = \frac{W}{\pi^2 R E^*} \left(\ln \frac{16\rho}{b} - \frac{1}{2} \right) \quad (8)$$

Basically, Argatov's model is the same as Greenwood's model. Oka's model is too complicated, and must be evaluated numerically. Gui et al. employed two-dimensional Hertz contact, but used wrong assumption ($b^2 = 2\rho b$). Zhao and Talke's use Johnson's equation for contact between a cylinder (Johnson, 1985), but obtained a wrong form (ρ/b) in equation (8). Thus, Greenwood's model is used in this paper.

3. Finite Element Analysis

In this paper, finite element analysis is employed.

The following parameters are used.

$$\rho = 50\mu\text{m}, E = 200 \text{ GPa}, \nu = 0.3.$$

$$R = 5\mu\text{m}, 10\mu\text{m}, 20\mu\text{m}, 50\mu\text{m}.$$

Totally, four cases are simulated.

Boundary conditions are shown in Figure 2. The half-space is represented by a large cylinder with height and radius equal to $250\mu\text{m}$. The annular donut-shaped asperity is set to be rigid. The left side is the axisymmetric axis. The bottom is fixed. The donut-shaped asperity is pressed downward $0.5\mu\text{m}$ ($\delta/\rho = 0.01$). Quasi-static analysis is employed in the finite element analyses.

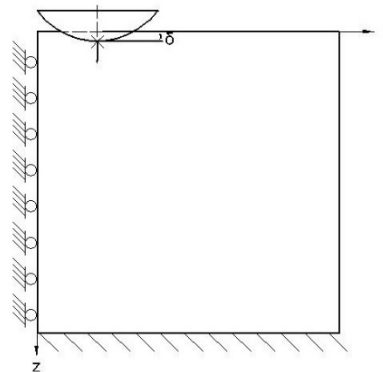


Figure 2. The boundary conditions.

$$\delta/\rho = 0.01.$$

Result

Figure 3a shows the complete deflection curves of the cross section for $R = 5\mu m$, $\rho = 50\mu m$ and $\delta = 0.5\mu m$ ($\delta/\rho = 0.01$ and $R/\rho = 0.1$). Figure 3b shows the contact pressure distribution. Figure 3c shows the coordinates of the outer and the inner edges of the contact (denoted as r_{in} and r_{out}). From these figures, it is obvious that Greenwood's prediction is not accurate.

In Fig. 3b, it is found that the coordinate of p_0 (denoted as R_{max}) is larger than R . The magnitude of p_0 is larger than that of the two-dimensional Hertz contact. In Fig. 3c, both the coordinates of the outer and the inner contact edges are larger than those of the two-dimensional Hertz contact. The contact edges are not symmetric about either R or R_{max} . Define the inner half-width b_{in} as $R_{max} - r_{in}$, and the outer half-width b_{out} as $r_{out} - R_{max}$. b_{in} is larger than b_{out} .

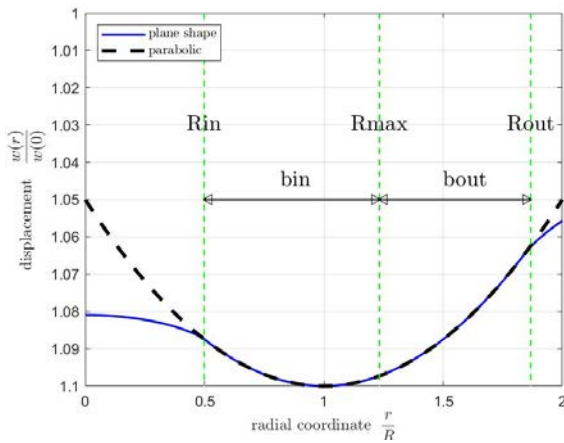


Figure 3a. Complete deflection curves for $R/\rho = 0.1$ and $\delta/\rho = 0.01$.

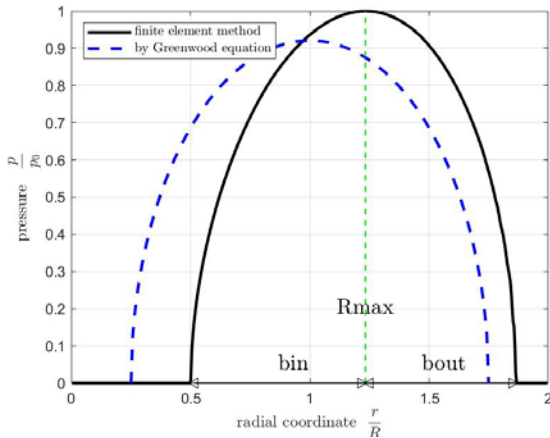


Figure 3b. Pressure distribution for $R/\rho = 0.1$ and $\delta/\rho = 0.01$

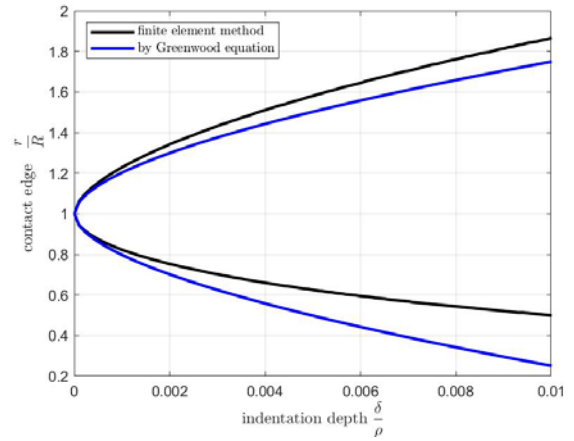


Figure 3c. Contact edges vs indentation depth for $R/\rho = 0.1$.

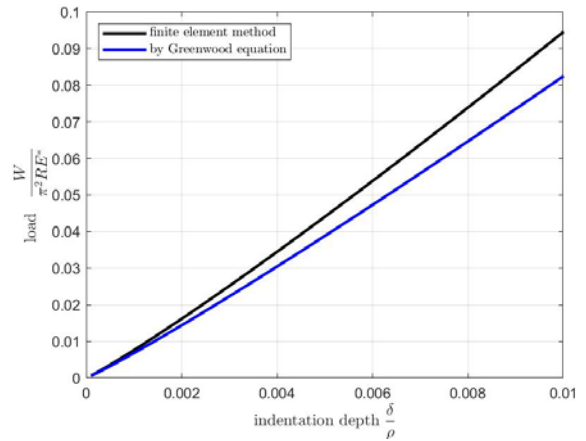


Figure 4. Load vs. indentation depth for $R/\rho = 1$ and $\delta/\rho = 0.01$.

Figure 4 shows load vs indentation depth for $R/\rho = 1$ and $\delta/\rho = 0.01$. It is found that Greenwood's prediction underestimates the total load. Therefore, Greenwood's model needs to be modified.

Discussion

1. Comparison with Greenwood's prediction

Both Argatov (2016) and Greenwood (2001) assumed that the maximum pressure is at $r = R$, the contact half-width is b , and the pressure distribution follows equation (1). Based on these assumptions, equation (2) is derived. Then, Greenwood used two-dimensional Hertz contact (equations (3) and (4)), and derived equations (5) and (6).

From Fig. 3a, the maximum deflection is at $r = R$. But, from Fig. 3b, the the maximum pressure is at $r = R_{max}$ ($R_{max} > R$). The magnitude of the maximum pressure p_0 is larger than that of two-dimensional Hertz contact. The pressure distribution is different from equation (1). Also from Fig. 3c, the inner half-width b_{in} is not the same as the outer half-width b_{out} . The inner and outer radii are different from that of the two-dimensional Hertz contact. Thus, in Fig. 4, the non-dimensional load vs. indentation depth are different from Greenwood's equations.

2. Modification equations

Since the contact is different from two-dimensional Hertz contact, following modified equations are proposed.

2.1 Maximum pressure

(1) Coordinate at maximum pressure

The coordinate of the maximum pressure is R_{max} not at R . As the δ is larger, R_{max} is larger. The coordinate at the maximum pressure can be fitted by the simulated results. The semi-empirical formulas for the coordinate of the maximum pressure is listed in Table 1.

$\frac{R}{\rho}$	fitting equation for $\frac{R_{max}}{R}$	maximum error
0.1	$\frac{R_{max}}{R} = -992.9 \left(\frac{\delta}{\rho}\right)^2 + 33.06 \left(\frac{\delta}{\rho}\right) + 1$	0.69%
0.2	$\frac{R_{max}}{R} = -23.87 \left(\frac{\delta}{\rho}\right)^2 + 9.075 \left(\frac{\delta}{\rho}\right) + 1$	0.39%
0.4	$\frac{R_{max}}{R} = -10.62 \left(\frac{\delta}{\rho}\right)^2 + 2.845 \left(\frac{\delta}{\rho}\right) + 1$	0.1%
1	$\frac{R_{max}}{R} = -8.296 \left(\frac{\delta}{\rho}\right)^2 + 0.4833 \left(\frac{\delta}{\rho}\right) + 1$	0.06%

Table 1. Fitting parameters for R_{max}/R .

For the same R/ρ , as δ/ρ is larger, R_{max}/R is larger. For the same δ/ρ , as R/ρ is smaller, R_{max}/R is larger. For example, at $\delta/\rho = 0.01$, $R_{max}/R=1.32$ for $R/\rho = 0.1$, and $R_{max}/R=1.005$ for $R/\rho = 1$. As R/ρ is large, R_{max} is nearly equal to R .

(2) Magnitude of the maximum pressure

In two-dimensional Hertz contact, the maximum pressure depends on the radius of the cylinder and the width.

$$p_0 = \frac{bE^*}{2\rho} \tag{9}$$

However, the donut-shaped asperity is annular. The maximum pressure is larger than that of the two-dimensional Hertz contact. Therefore, there is a correction factor K_1 for p_0 . Define the half-width b as the average of the inner half-width and the out half-width.

$$b = \frac{b_{in}+b_{out}}{2} \tag{10}$$

The maximum pressure should be that of two-dimensional Hertz contact corrected by a factor K_1 .

$$p_0 = K_1 \frac{bE^*}{2\rho} \tag{11}$$

The semi-empirical equation for the factor K_1 is shown in table 2.

$\frac{R}{\rho}$	fitting equation for K_1 .	maximum error
0.1	$K_1 = -757.8 \left(\frac{\delta}{\rho}\right)^2 + 26.65 \left(\frac{\delta}{\rho}\right) + 1$	0.4%
0.2	$K_1 = -26.04 \left(\frac{\delta}{\rho}\right)^2 + 7.876 \left(\frac{\delta}{\rho}\right) + 1$	0.37%
0.4	$K_1 = 150.6 \left(\frac{\delta}{\rho}\right)^2 + 1.032 \left(\frac{\delta}{\rho}\right) + 1$	0.4%
1	$K_1 = 327.9 \left(\frac{\delta}{\rho}\right)^2 - 2.417 \left(\frac{\delta}{\rho}\right) + 1$	0.49%

Table 2. Fitting parameters for K_1

For the same R/ρ , as δ/ρ is larger, K_1 is larger. For the same δ/ρ , as R/ρ is smaller, K_1 is larger. For example, at $\delta/\rho = 0.01$, $K_1=1.2$ for $R/\rho = 0.1$, and $K_1=1.008$ for $R/\rho = 1$. As R/ρ is large, K_1 is nearly equal to 1.

(3) Pressure distribution

Thus, the pressure distribution can be approximated by

$$p = \frac{p_0}{b_{in}} \sqrt{b_{in}^2 - (r - R_{max})^2} \quad \text{for } R_{max} - b_{in} \leq r \leq R_{max} \tag{12}$$

$$p = \frac{p_0}{b_{out}} \sqrt{b_{out}^2 - (r - R_{max})^2} \quad \text{for } R_{max} + b_{out} \geq r \geq R_{max} \tag{13}$$

The pressure distribution can be approximation by equations (12) and (13) with tolerable error. Figure 5 shows the modified pressure.

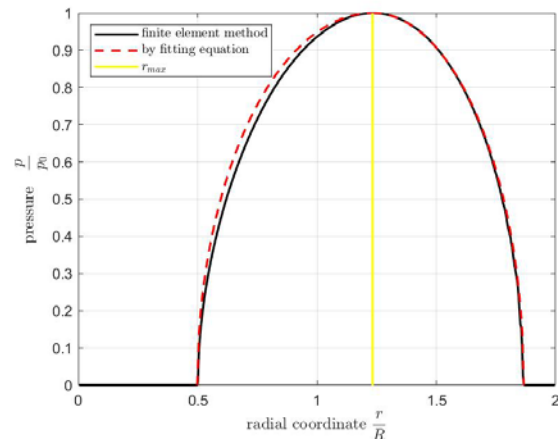


Figure 5. Fitted pressure distribution for $R/\rho = 0.1$

and $\delta/\rho = 0.01$.

2.2 Total load and maximum pressure

In two-dimensional Hertz contact,

$$W = \pi^2 R b p_0 \tag{14}$$

Since the donut-shaped asperity is annular, the total contact force is different from a cylinder. Therefore, there should be a correction factor K_2 for total load.

$$W = K_2 \pi^2 R_{max} b p_0 \tag{15}$$

The factor is shown in Table 3.

$\frac{R}{\rho}$	fitting equation for K_2	maximum error
0.1	$K_2 = 833.9 \left(\frac{\delta}{\rho}\right)^2 - 14.16 \left(\frac{\delta}{\rho}\right) + 1$	0.32%
0.2	$K_2 = 317.3 \left(\frac{\delta}{\rho}\right)^2 - 7.569 \left(\frac{\delta}{\rho}\right) + 1$	0.50%
0.4	$K_2 = 326.4 \left(\frac{\delta}{\rho}\right)^2 - 5.653 \left(\frac{\delta}{\rho}\right) + 1$	0.47%
1	$K_2 = 411.4 \left(\frac{\delta}{\rho}\right)^2 - 5.363 \left(\frac{\delta}{\rho}\right) + 1$	0.49%

Table 3. Fitting parameters for K_2 .

For the same R/ρ , as δ/ρ is larger, K_2 is smaller. For the same δ/ρ , as R/ρ is smaller, K_2 is larger. For example, at $\delta/\rho = 0.01$, $K_2 = 0.94$ for $R/\rho = 0.1$, and $K_2 = 0.99$ for $R/\rho = 1$.

The total load can be obtained as

$$W = K_1 K_2 \pi^2 \frac{R_{max} b^2 E^*}{2\rho} \tag{16}$$

2.3 Indentation depth and half-width

Both Argatov (2016) and Greenwood (2001) derived the following equation.

$$\delta = \frac{b p_0}{E^*} \left(\ln \frac{16R}{b} + \frac{1}{2} \right) \tag{2}$$

This equation is based on the assumption that, the maximum pressure is located at R , the half-width is b , and the pressure distribution follows equation (1). The constant 1/2 is obtained by integrating the pressure distribution.

In the finite element analysis, the pressure distribution does not follow equation (1), therefore, the constant is different from 1/2. In order to find the inner half-width and the outer half-width, the equation can be modified. As Gui et al.'s research, the constant may be different from 0.5. It is reasonable to assume there are different constants for the contact with different half-widths. Thus, equation (2) can be modified as the following equations.

$$\delta = \frac{W}{\pi^2 R E^*} \left(\ln \frac{16R}{b_{in}} + C_{in} \right) \tag{17}$$

$$\delta = \frac{W}{\pi^2 R E^*} \left(\ln \frac{16R}{b_{out}} + C_{out} \right) \tag{18}$$

$$\delta = \frac{W}{\pi^2 R E^*} \left(\ln \frac{16R}{b} + C \right) \tag{19}$$

Using the simulation results, the C_{in} , C_{out} and C are listed in Table 4.

$\frac{R}{\rho}$	C_{in}	C_{out}	C
0.1	0.2921	0.8385	0.6028
0.2	0.2453	0.6122	0.4454
0.4	0.061	0.304	0.1899
1	-0.3658	-0.2375	-0.2996

Table 4. Constant for inner and outer half-width.

If the mean half-width is used, equation (19) can be transformed into the following equation.

$$\delta = \frac{K_1 K_2 b^2}{2\rho} \left(\ln \frac{16R}{b} + C \right) \tag{20}$$

Given δ , ρ and R , the contact half-width b can be obtained from equation (20) by iteration. Total load can be obtained from equation (16). Then, b_{in} and b_{out} can be obtained by equations (17) and (18). Figure 6 shows that the coordinates of contact edges vs. indentation depth. The modified equations can predict the coordinates of the contact edges very accurately.

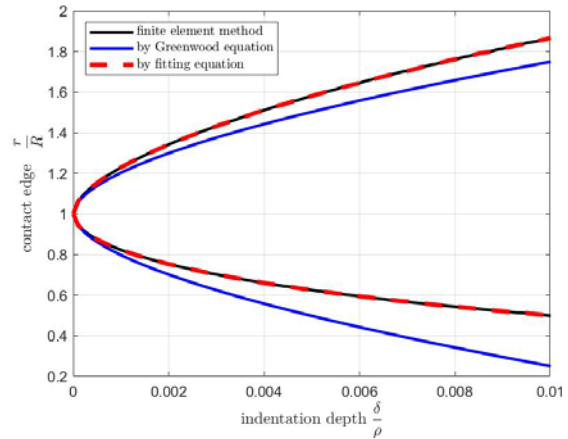


Figure 6. Coordinates of the contact edges vs. indentation depth for $R/\rho = 0.1$ and $\delta/\rho = 0.01$.

2.4 Total Load and indentation depth

Using equations (18), the indentation depth can be obtained. Then, total load can be obtained from equation (12). Figure 7 shows the relationship between total load and indentation depth for $R/\rho = 1$ and $\delta/\rho = 0.01$. Greenwood's equation cannot predict the load accurately. Equations (18) or (12) can predict the load very accurately.

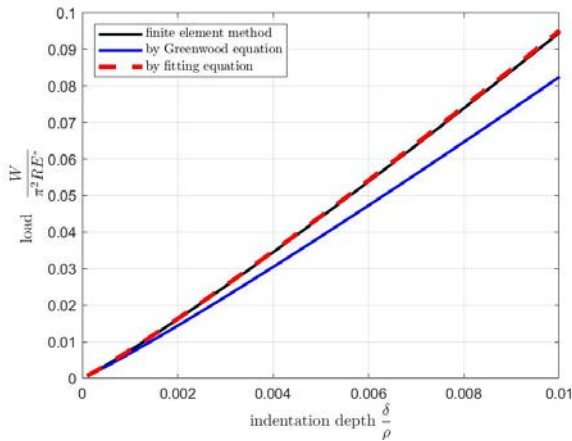


Figure 7. Load vs. indentation depth for $R/\rho = 1$ and $\delta/\rho = 0.01$.

3 Summary

The donut contact can be described by two-dimensional Hertz contact modified by K_1 , K_2 , C , R_{max} .

Given ρ , R and δ , R_{max} can be obtained from table 1. K_1 and K_2 can be obtained from table 2 and 3, respectively. b can be obtained from equation (19) by iteration. Then, p_0 can be obtained from equation (14), and W can be obtained from equation (12). b_{in} and b_{out} can be obtained from equations (17) and (18). Fig. 5 to 7 show that the modified equations can predict the contact accurately.

Argatov et al. (2016) showed that their model is in the leading approximation. Popov et al. (2019) showed that this model is only valid for “thin ring” (i.e. $b \ll R$). From the results, it is obvious that, as R/ρ is large, the contact point is nearly located at the central line. Greenwood and Argatov et al.’s model is applicable. As R/ρ is small, the contact point is not located at the central line. The assumption is no longer true, and the modified model is necessary.

Conclusion

The contact between a donut-shaped asperity and a half-space is analyzed using finite element method. The result is compared with Greenwood’s prediction based on two-dimensional Hertz contact. It is found that Greenwood’s prediction is accurate. The modified equations are proposed. The contact for a donut-shaped asperity can be approximated by the modified equations.

Reference

Argatov, I.I., Li, Q., Pohrt, R., Popov, V.L., “Johnson–Kendall–Roberts adhesive contact for a toroidal indenter,” Proc. R. Soc. London Ser. A, Vol. 472, 20160218 (2016).
 Argatov, I.I. and Nazarov, S.A., “The contact problem

for a narrow annular punch. Increasing contact zone,” In: Studies in elasticity and plasticity, pp. 15–26, University Press, St. Petersburg (1999).

Bhaduria, D., Batala, A., Dimova, S.S., Zhangb, Z., Dongb, H., Fallqvistc, M. and M’Saoubid, R., “On design and tribological behaviour of laser textured surfaces,” Procedia CIRP, Vol. 60, 20 – 25, (2017).
 Dou, L., Yang, L., Wang, S., Zhang, B., Zhu, W., Jiang, Y., Yu, Z., Wu, Q., “Dry friction and wear behavior of volcano arrays based mixed morphology textured by femtosecond laser”, Materials Today Communications, Vol. 34. 105093 (2023).
 Greenwood, J.A., “Elastic contact with a donut-shaped asperity,” International Journal of Mechanical Sciences, Vol. 43, pp. 1473-1482, (2001).
 Gui J, Kuo D, Marchon D, Rauch GC. “A stiction model for a head-disk interface,” IEEE Transactions on Magnetics, Vol. 34, pp. 932-937 (1997).
 Johnson, K.L., Contact mechanics, Cambridge: Cambridge University Press (1985).
 Kelley, J., Babaalihaghighi, K., Bader, N., Wege, C., Pape, F., Poll, G., “Application of Hertzian theory to torus on plane contacts”, Proc IMechE Part J: Engineering Tribology, Vol. 236, No. 11, pp. 2189–2208 (2022).
 Oka M., “Stiction problem of annular-shaped laser textured bump on a hard disk,” Tribology International, Vol. 33, pp. 353-356 (2000).
 Popov, V.L., Heß, M., Willert, E., “Annular contacts”, in Handbook of Contact Mechanics, Springer Berlin (2019).
 Zhao Q, Talke F., “Plasticity index for contact between a head and a disk with crater-shaped laser bumps,” Journal of Tribology, Vol. 122 (1), pp. 269-273 (2000).

Nomenclature

b the contact half-width at cross section of the asperity.

b_{in} inner half-width, $b_{in} = R_{max} - r_{in}$

b_{out} outer half-width, $b_{out} = r_{out} - R_{max}$

C, C_{in}, C_{out} constants in equations for δ .

E Young’s modulus.

E^* equivalent Young’s modulus, $E^* = (1 - \nu^2)/E$

K_1 a factor, $p_0 = K_1 \frac{bE^*}{2\rho}$

K_2 a factor, $W = K_2 \pi^2 R_{max} b p_0$

p pressure

p_0 maximum pressure

R the radius of the annular donut-shaped asperity.

R_{max} coordinate of the maximum pressure.

r radial coordinate

r_{in} coordinate of the inner edge of the contact.

r_{out} coordinate of the outer edge of the contact.

W total load

δ indentation depth of the donut-shaped asperity

ν Poisson ratio

ρ radius of curvature at the cross section of the donut-shaped asperity.

甜甜圈型坡峰與半平面彈性接觸之有限元素分析

吳俊仲 吳佳鴻

長庚大學機械工程學系 台灣大學應用力學研究所

摘要

過去二十年，許多學者使用赫茲接觸研究甜甜圈型坡峰的接觸問題。本研究直接使用有限元素法研究甜甜圈型坡峰的接觸問題。結果顯示，二維赫茲接觸並非很好的近似。本研究提出半經驗公式，可以精確預測合力、下壓深度與合力的關係，接觸半寬度等參數。